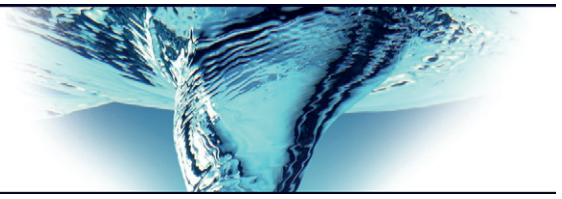
J. Fluid Mech. (2019), *vol.* 878, R1, doi:10.1017/jfm.2019.667



JFM RAPIDS
journals.cambridge.org/rapids

Universal fluctuations in the bulk of Rayleigh–Bénard turbulence

Yi-Chao Xie[1,2,†], Bu-Ying-Chao Cheng[1], Yun-Bing Hu[1,2] and Ke-Qing Xia[1,2,†]

[1]Department of Physics, The Chinese University of Hong Kong, Shatin, Hong Kong, PR China

[2]Center for Complex Flows and Soft Matter Research & Department of Mechanics and Aerospace Engineering, Southern University of Science and Technology, Shenzhen, 518055, PR China

(Received 25 June 2019; revised 9 August 2019; accepted 9 August 2019;
first published online 6 September 2019)

We present an investigation of the root-mean-square (r.m.s.) temperature σ_T and the r.m.s. velocity σ_w in the bulk of Rayleigh–Bénard turbulence, using new experimental data from the current study and experimental and numerical data from previous studies. We find that, once scaled by the convective temperature θ_*, the value of σ_T at the cell centre is a constant ($\sigma_{T,c}/\theta_* \approx 0.85$) over a wide range of the Rayleigh number ($10^8 \leqslant Ra \leqslant 10^{15}$) and the Prandtl number ($0.7 \leqslant Pr \leqslant 23.34$), and is independent of the surface topographies of the top and bottom plates of the convection cell. A constant close to unity suggests that θ_* is a proper measure of the temperature fluctuation in the core region. On the other hand, $\sigma_{w,c}/w_*$, the vertical r.m.s. velocity at the cell centre scaled by the convective velocity w_*, shows a weak Ra-dependence ($\sim Ra^{0.07\pm0.02}$) over $10^8 \leqslant Ra \leqslant 10^{10}$ at $Pr \sim 4.3$ and is independent of plate topography. Similar to a previous finding by He & Xia (*Phys. Rev. Lett.*, vol. 122, 2019, 014503), we find that the r.m.s. temperature profile $\sigma_T(z)/\theta_*$ in the region of the mixing zone with a mean horizontal shear exhibits a power-law dependence on the distance z from the plate, but now the universal profile applies to both smooth and rough surface topographies and over a wider range of Ra. The vertical r.m.s. velocity profile $\sigma_w(z)/w_*$ obeys a logarithmic dependence on z. The study thus demonstrates that the typical scales for the temperature and the velocity are the convective temperature θ_* and the convective velocity w_*, respectively. Finally, we note that θ_* may be utilised to study the flow regime transitions in ultrahigh-Ra-number turbulent convection.

Key words: Bénard convection, turbulent convection

1. Introduction

Rayleigh–Bénard convection (RBC), a fluid layer confined between two plates heated from below and cooled from above, continues to attract attention not only

† Email addresses for correspondence: ycxie@cuhk.edu.hk, xiakq@sustech.edu.cn

© Cambridge University Press 2019

https://doi.org/10.1017/jfm.2019.667 Published online by Cambridge University Press

because of its relevance to geophysical and astrophysical flows, but also owing to the fact that it is an idealised model for the study of thermally driven turbulence (for reviews, see, for example, Ahlers, Grossmann & Lohse (2009), Lohse & Xia (2010), Chillà & Schumacher (2012), Xia (2013)). In RBC, buoyancy injects energy into the turbulence and creates vigorous velocity and temperature fluctuations. Understanding the dynamics of these fluctuations has been one of the central issues (Grossmann & Lohse 2004). The RBC system is controlled by two dimensionless parameters – the Rayleigh number $Ra = \alpha g \Delta T H^3/(\kappa\nu)$ and the Prandtl number $Pr = \nu/\kappa$, where g is the gravitational acceleration constant, H the height of the convection cell, ΔT the temperature difference across the top and bottom plates, and α, κ and ν are the thermal expansion coefficient, the thermal diffusivity and the kinematic viscosity of the working fluid, respectively.

Two turbulence states with different probability density functions (PDFs) of the temperature at the cell centre were observed in turbulent RBC – a 'soft turbulence' state with a Gaussian PDF and a 'hard turbulence' state with an exponential PDF (Heslot, Castaing & Libchaber 1987). In the latter, the r.m.s. temperature σ_T normalised by ΔT obeys a -0.145 power law with Ra. A mixing-length model was proposed to explain this dependence (Castaing *et al.* 1989). However, later studies show that $\sigma_T/\Delta T$ not only depends on Pr but also on the plate topography, even for the most widely studied aspect-ratio-unity cylindrical cells (see table 1 for a summary). It is thus natural to ask if there is any universal behaviour of the temperature fluctuations in the bulk flow.

In addition to the value of σ_T at the cell centre, the functional form of the root-mean-square (r.m.s.) temperature profile $\sigma_T(z)$ is also of great interest as its shape determines the transport properties across the boundary. Based on different assumptions of the local force balance, theory predicts different profiles of $\sigma_T(z)$ (Adrian 1996). Only very recently, a clear understanding of $\sigma_T(z)$ has been obtained (He & Xia 2019): while in a region with mean horizontal shear (the viscous force balances the inertia force), $\sigma_T(z)$ obeys a power-law dependence on z; in regions with abundant plume emissions (the buoyancy balances the inertia force), $\sigma_T(z)$ is in a logarithmic form, which is true for the idealised case – that is, turbulent RBC in cells with smooth surfaces ('smooth cell'). In the presence of roughness on the top and bottom boundaries ('rough cell'), σ_T is enhanced considerably (Du & Tong 2001). An interesting question is whether σ_T shows universal behaviour in cells with different plate topographies. In addition to the shape of $\sigma_T(z)$, there is no generally accepted characteristic temperature scale in the bulk. For instance, ΔT has been widely used as a typical temperature scale, but the maximum value $\sigma_T(z)_{max}$ is also used sometimes (see, for example, Wang *et al.* (2018)). The Ra-dependence of $\sigma_T(z)$ scaled by different scales exhibits different features: while $\sigma_T(z)/\Delta T$ for different Ra differs (Sun, Cheung & Xia 2008; Ahlers *et al.* 2012), $\sigma_T(z)/\sigma_T(z)_{max}$ for different Ra collapses better in the mixing zone. Therefore, the typical temperature scale in the bulk is not clear at present.

Compared to numerous studies on temperature fluctuations, the investigation on velocity fluctuations in turbulent RBC is scarce. The velocity fluctuation is usually studied in terms of a Reynolds number based on the vertical r.m.s. velocity σ_w, given by $Re_{\sigma_w} = \sigma_w H/\nu$. It is found that Re_{σ_w} scales with Ra to a 0.5 power law, consistent with the free-fall-like argument (Shen, Xia & Tong 1995; Daya & Ecke 2001; Qiu *et al.* 2004; Shang, Tong & Xia 2008). To the best of our knowledge, there have been almost no direct measurements of velocity fluctuations in rough cells. The typical velocity scale in the bulk flow also remains to be explored.

https://doi.org/10.1017/jfm.2019.667 Published online by Cambridge University Press

Ref.	Ra	Pr	A	γ	Geometry	Surface type
(*a*)	$1.2\times10^8\sim6.5\times10^{10}$	0.7	0.36	−0.147	Cylinder	*S*
(*b*)	$7.7\times10^7\sim1.0\times10^{15}$	0.7	0.37	−0.145	Cylinder	*S*
(*c*)	$4.8\times10^8\sim5.8\times10^9$	5.4	0.192	−0.14	Cylinder	*R*
(*d*)	$2.5\times10^8\sim3.9\times10^9$	5.46	N/A	−0.10	Cylinder	*S*
(*d*)	$2.5\times10^8\sim3.9\times10^9$	5.46	N/A	−0.48	Cube	*S*
(*e*)	$5.7\times10^8\sim1.1\times10^{10}$	7	5.9	−0.35	Cube	*S*
(*f*)	$1.0\times10^7\sim2.0\times10^9$	5.2	N/A	−0.18	Cylinder	*S*
(*g*)	$3.6\times10^8\sim7.6\times10^9$	4.3	$0.066\sim0.10$	−0.1	Cylinder	*S* and *R*
(*h*)	$3.0\times10^7\sim3.0\times10^9$	4.3	9.38	−0.35	Cube	*S*
(*i*)	$1.0\times10^{11}\sim4.2\times10^{11}$	12.3	N/A	−0.17	Cylinder	*S*
(*j*)	$4.0\times10^9\sim1.3\times10^{11}$	23.34	0.08	−0.09	Cylinder	*R*
Present	$1.6\times10^8\sim8.8\times10^9$	4.3	$0.001\sim0.12$	$-0.10\sim0.12$	Cylinder	*S* and *R*

TABLE 1. Scaling of the r.m.s. temperature ($\sigma_{T,c}/\Delta T = ARa^{\gamma}$) at the cell centre. In the surface type column, '*S*' stands for 'smooth surface cell' and '*R*' stands for 'rough surface cell'. The references are: (*a*) Castaing *et al.* (1989), (*b*) Niemela *et al.* (2000), (*c*) Du & Tong (2001), (*d*) Daya & Ecke (2001), (*e*) Wang & Xia (2003), (*f*) Lakkaraju *et al.* (2012), (*g*) Wei *et al.* (2014), (*h*) Kaczorowski, Chong & Xia (2014), (*i*) Wei & Ahlers (2016); (*j*) Xie & Xia (2017).

In this paper, we present an investigation of the temperature and the velocity fluctuations in the bulk of turbulent RBC. We demonstrate that the typical temperature and velocity scales in the bulk are, respectively, the convective temperature θ_* and the convective velocity w_*. Once scaled by these quantities, the fluctuations in the bulk exhibit universal behaviour. These findings shed new light on the bulk dynamics in convective turbulence.

2. The experimental set-up and relevant parameters

The experiment was carried out in an upright cylindrical cell with an aspect ratio $\Gamma = D/H \approx 1$, where $D = 192$ mm is the cell diameter and $H = 202$ mm is its height. The design and construction of the cell can be found in Xie & Xia (2017). We mention only its essential features here. The cell consists of three parts: a copper top plate, a copper bottom plate and a Plexiglas sidewall. The bottom plate was heated by rubber electrical heaters and the top plate was cooled by passing temperature-controlled water through a chamber fitted onto its top surface. The temperature of the top (bottom) plate was measured using four (five) thermistors, from which we calculated Ra, Pr and the Nusselt number $Nu = QH/(\chi\Delta T)$, where Q is the heat flux supplied at the bottom plate and χ the thermal conductivity of the fluid. Deionised and degassed water was used as the working fluid, with a mean fluid temperature kept at a constant of 40 °C. Thus the Prandtl number was $Pr = 4.34$. By changing ΔT, we achieved a Ra range of $1.59\times10^8 \leqslant Ra \leqslant 8.82\times10^9$. To study the effects of wall roughness on the fluctuations of the temperature and the velocity, another set of measurements in a rough cell were made. The roughness elements were in the form of square-latticed pyramids with a height h of 8 mm. The heat transport in rough cells shows three regimes depending on Ra (Xie & Xia 2017). The Ra range in the present study in the rough cell is in the heat-transport-enhanced regimes.

The r.m.s. temperature, $\sigma_T = \sqrt{\langle (T - \langle T\rangle)^2\rangle}$, inside the cell was measured using a waterproof thermistor with a head diameter of 0.3 mm and a response time of

https://doi.org/10.1017/jfm.2019.667 Published online by Cambridge University Press

30 ms, where $\langle\cdots\rangle$ stands for time averaging. Two sets of temperature fluctuation measurements were made. In the first set, the r.m.s. temperature at the centre $\sigma_{T,c}$ of the smooth cell and the rough cell were measured as a function of Ra. In the second set, the vertical r.m.s. temperature profiles $\sigma_T(z)$ were measured in the rough cell. The location of $z = 0$ mm was set at the valley of the roughness elements on the bottom plate. At each vertical position z, a temperature time trace was measured for one hour with a sampling rate of 15 Hz. Good care was taken to ensure that the system was isolated from the surrounding temperature variations. For the detailed thermal isolation method, we refer to Xie, Ding & Xia (2018).

The vertical velocity fluctuation, characterised by a Reynolds number $Re_{\sigma_w} = \sigma_w H/\nu$, was measured at the centre of the rough cell, using a laser Doppler velocimeter (LDV). Here $\sigma_w = \sqrt{\langle (w - \langle w\rangle)^2\rangle}$ is the vertical r.m.s. velocity. The flow was seeded with tracer particles with a diameter of 2.893 μm. The LDV sampling rate was ∼30 Hz. Typical measurements lasted for 12 h to obtain sufficient statistics of the second-order quantity like the r.m.s. velocity.

Considering the region outside the boundary layers, the relevant physical parameters governing the flow dynamics are αg, Q_0 and H, where $Q_0 = Q/(\rho c_p)$ is the specific heat flux, and ρ and c_p are, respectively, the density and the specific heat capacity of the working fluid. A simple dimensional analysis yields the convective temperature θ_* and the convective velocity w_*: $\theta_* \equiv Q_0^{2/3}/(\alpha g H)^{1/3}$ and $w_* \equiv (\alpha g H Q_0)^{1/3}$ (Deardorff 1970). The two scales can be expressed in dimensionless forms in terms of Ra, Pr and Nu as

$$\theta_*/\Delta T = Nu^{2/3}/(RaPr)^{1/3}, \quad Re_{w_*} = w_* H/\nu = (RaNuPr^{-2})^{1/3}. \tag{2.1a,b}$$

3. Results and discussions

3.1. *The temperature fluctuation in the bulk*

We first study the r.m.s. temperature profiles. Figures 1(*a*) and 1(*c*) show $\sigma_T(z)$ normalised, respectively, by the temperature difference across the top and bottom plates (ΔT) and the convective temperature (θ_*) measured in the rough cell for $Ra = 3.2 \times 10^8$, 2.2×10^9 and 5.2×10^9. The r.m.s. temperatures ($\sigma_{T,c}$) measured at the centre of the smooth cell for $8.9 \times 10^8 \leqslant Ra \leqslant 9.3 \times 10^9$ are plotted as hexagons. For comparison, we also plot in these figures $\sigma_T(z)$ measured in smooth cells from Du & Tong (2000) at $Ra = 1.5 \times 10^9$ and from Wei *et al.* (2014) at $Ra = 6.8 \times 10^8$. The horizontal axes are normalised by H.

It is seen that the profiles measured in either a smooth cell or a rough cell for different Ra collapse onto each other outside the thermal boundary layer (TBL). With increasing z, $\sigma_T(z)$ increases to a maximum and then decreases gradually when moving towards the cell centre. These observations are in general consistent with earlier studies (see, for example, Lui & Xia (1998)). However, considerable differences between $\sigma_T(z)/\Delta T$ measured in smooth cells and in rough cells are observed (figure 1*a*). First, the outer edge of the TBL (that is, the peak position of $\sigma_T(z)/\Delta T$) is shifted towards the cell centre, which is because the motionless fluids trapped in the bottom of valleys between roughness elements have very small temperature fluctuations. Second, σ_T is enhanced considerably near the edge of the TBL in rough cells owing to more thermal plumes being emitted from the tip of

https://doi.org/10.1017/jfm.2019.667 Published online by Cambridge University Press

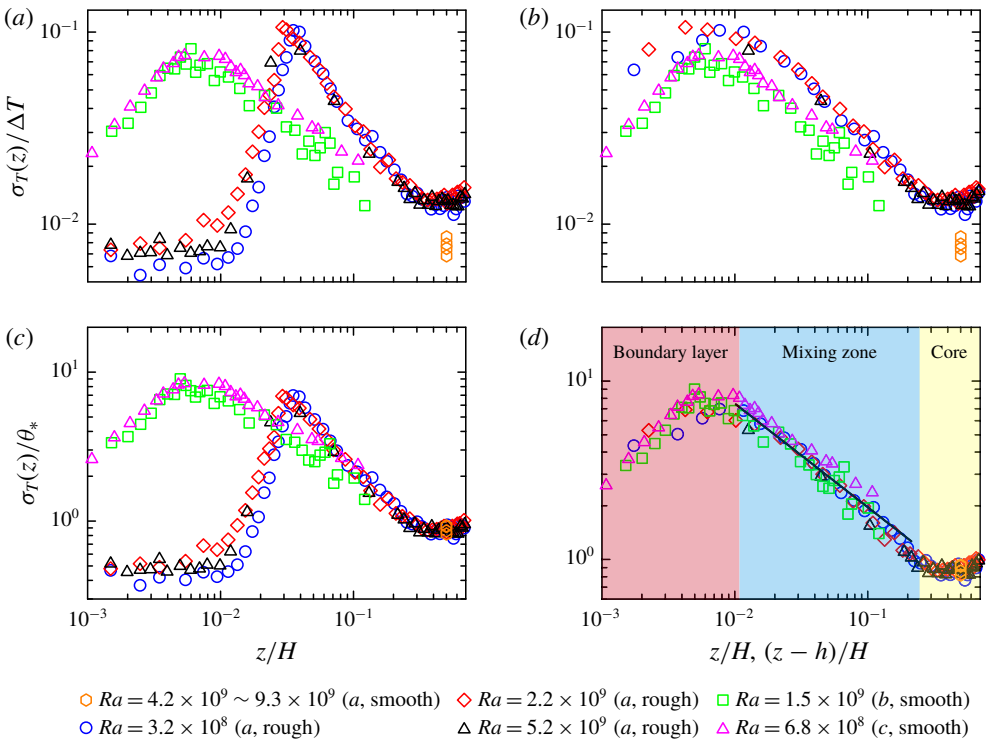


FIGURE 1. Measured r.m.s. temperature profiles $\sigma_T(z)$ along the cell centreline. The vertical axis is scaled by ΔT (a,b) and by θ_* (c,d). The horizontal axes are scaled by the cell height H. The legends with 'smooth' and 'rough' stand for smooth cells and rough cells, respectively. In (b,d), the distance z for the data measured in the rough cell is offset by the roughness height h. The solid line in (d) is a power-law fit to the data in the range $10^{-2} \leqslant z/H \leqslant 2 \times 10^{-1}$ given by $\sigma_T/\theta_* = 0.53 \times (z/H)^{-0.57\pm0.03}$. The data sources are ($a$) present, ($b$) Du & Tong (2000) and ($c$) Wei *et al.* (2014).

roughness elements. This enhancement is also true at the cell centre since the data in the smooth cell are systematically smaller than those in the rough cell. However, we note, even for a smooth cell, Ahlers *et al.* (2012) showed that $\sigma_T(z)/\Delta T$ for different Ra does not collapse in the classical regime of turbulent RBC. The above results suggest that ΔT is not a suitable characteristic scale for σ_T. When scaled with θ_*, the r.m.s. temperature at the cell centre, for both the smooth and the rough cells, collapse onto each other (but not for the profile in the mixing zone), and the magnitude of the fluctuation at the edge of the TBL also becomes comparable in two cases (figure 1c). To compare directly the r.m.s. temperature profiles in the bulk region, in figure 1(b,d), the distance z of the data measured in the rough cells is offset by the roughness height h. Remarkably, compared with $\sigma_T(z)/\Delta T$ (figure 1b), $\sigma_T(z)/\theta_*$ in smooth and rough cells collapse onto each other outside the TBL (figure 1d), suggesting that θ_* is a characteristic temperature scale in the bulk of turbulent convection.

We now examine the universal profiles shown in figure 1(d) in detail. They can be divided into three regions: a TBL region, a mixing zone and a core region, which are marked with different background colours. In the mixing zone spanning $3 \times 10^{-2} \leqslant z/H \leqslant 2.5 \times 10^{-1}$, a power law $\sigma_T/\theta_* = 0.53 \times (z/H)^{-0.57\pm0.03}$ fits the data nicely.

https://doi.org/10.1017/jfm.2019.667 Published online by Cambridge University Press

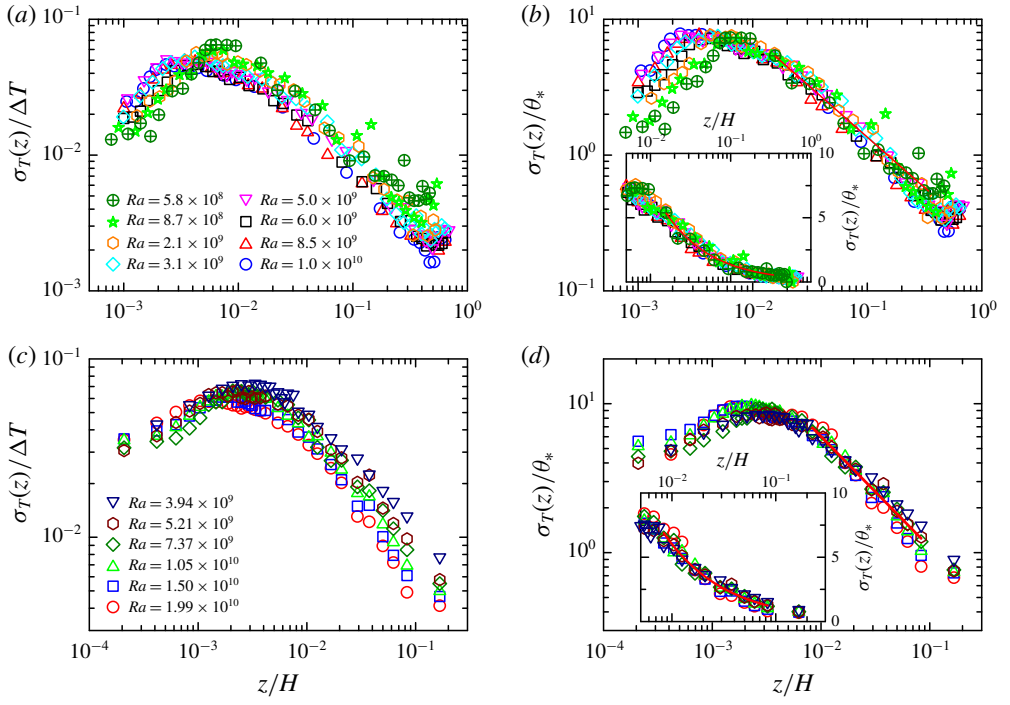


FIGURE 2. Measured r.m.s. temperature profiles along the centreline in a cubic cell (*a*,*b*) and in a rectangular cell (*c*,*d*). The vertical axes are normalised by ΔT (*a*,*c*) and by θ_* (*b*,*d*). The solid lines in (*b*,*d*) are power-law fits given by (*b*) $\sigma_T(z)/\theta_* = 0.25(z/H)^{-0.74\pm0.02}$ and (*d*) $\sigma_T(z)/\theta_* = 0.20(z/H)^{-0.74\pm0.02}$. Insets of (*b*,*d*): $\sigma_T(z)/\theta_*$ in linear–log plots. The data in the cubic cell are taken from Wang & Xia (2003) and those in the rectangular cell from Sun *et al.* (2008).

This scaling exponent is consistent with results in the literature (Wei & Ahlers 2016; Wang *et al.* 2018; He & Xia 2019), and also close to the theoretical prediction of $-1/2$ by Adrian (1996). This observation further supports that $\sigma_T(z)$ obeys a power-law decay in a region where a mean horizontal shear exists, and it is true for both smooth cells and rough cells. In the core region ($0.25 \leqslant z/H \leqslant 0.65$), $\sigma_T(z)/\theta_*$ is nearly a constant independent of Ra and the plate topography, suggesting a universal temperature fluctuation here.

We next test the convective temperature in other cell geometries. Figures 2(*a*) and 2(*b*) show $\sigma_T(z)$ normalised respectively by ΔT and θ_* measured along the centreline in a cubic cell. The r.m.s. temperature profiles obtained along the cell centreline in a rectangular cell are shown in figure 2(*c*,*d*). The data in the cubic cell are taken from Wang & Xia (2003) and those in the rectangular cell are from Sun *et al.* (2008). Let us focus on the cubic case first. It is seen that the originally Ra-dependent profiles (figure 2*a*) collapse onto each other once they are scaled by θ_* (figure 2*b*). The solid line in figure 2(*b*) is a power-law fit to the data in the range $2 \times 10^{-2} \leqslant z/H \leqslant 3 \times 10^{-1}$, yielding $\sigma_T(z)/\theta_* = 0.25(z/H)^{-0.74\pm0.02}$. Note that $\sigma_T(z)/\theta_*$ for different Ra do not collapse inside the TBL. This is because θ_* is a temperature scale for the bulk, so is not applicable in the near-wall region where the viscosity and the thermal diffusivity dominate the dynamics. Similar behaviour is observed in the

https://doi.org/10.1017/jfm.2019.667 Published online by Cambridge University Press

rectangular cell – that is, when compared with $\sigma_T(z)/\Delta T$, the $\sigma_T(z)/\theta_*$ data collapse better for different Ra, and can be fitted by a power law with a scaling exponent of -0.74 ± 0.02 in the mixing zone. The insets of figures 2(*b*) and 2(*d*) plot the same data as the main figures but in log–linear plots. They clearly show that these profiles cannot be fitted by logarithmic functions. Note that the scaling exponent is different from the cylindrical cells, suggesting that turbulent fluctuations in the bulk are cell-geometry-dependent, which may be partially attributed to the geometry dependence of the large-scale flow dynamics.

As σ_T/θ_* in the core region is a constant (figure 1*b*), we next focus on its value at the cell centre. Figure 3(*a*) plots $\sigma_{T,c}/\Delta T$ versus Ra measured in smooth cells and rough cells from the present study. For comparison, data for $\sigma_{T,c}/\Delta T$ adopted from a number of sources are also shown. These data span $10^7 \leqslant Ra \leqslant 10^{15}$ and $0.7 \leqslant Pr \leqslant 23.34$, and were measured in smooth cells and rough cells. Details about their Ra, Pr, scaling property and cell type can be found in table 1.

When scaled with ΔT, both the magnitude and the scaling property of $\sigma_{T,c}$ are seen to vary dramatically among different experiments (figure 3*a*). The data reveal that $\sigma_{T,c}/\Delta T$ generally decreases with Pr. The present measurements in rough cells even show a positive γ (that is, $\sigma_{T,c}/\Delta T \sim Ra^{0.1}$). Figure 3(*b*) plots the same data as those in figure 3(*a*), but scaled with θ_*, and figure 3(*c*) shows a zoomed region with $10^8 \leqslant Ra \leqslant 10^{12}$. To obtain $\sigma_{T,c}/\theta_*$, we first took published data of $\sigma_{T,c}/\Delta T$ as a function of Ra and Pr from the cited references, then calculated $\theta_*/\Delta T$ using (2.1*a*) with Ra, Pr and Nu that were measured together with $\sigma_{T,c}$. The ratio $(\sigma_{T,c}/\Delta T)/(\theta_*/\Delta T)$ is therefore $\sigma_{T,c}/\theta_*$.

We first look at data measured in cylindrical cells. It is seen that $\sigma_{T,c}/\theta_*$ from different experiments collapses around a straight line for $Ra > 1 \times 10^8$ (in the so-called 'hard turbulence' regime), suggesting the existence of a universal constant. The upper solid line in figure 3(*b*) marks the mean value ($\langle \sigma_{T,c}/\theta_* \rangle_{Ra,Pr} = 0.85$). A mean value close to unity suggests that θ_* is indeed a representative temperature in the core region. This universal constant indicates that a common mechanism governs temperature fluctuation dynamics in the core region.

For $\sigma_{T,c}/\theta_*$ measured in cubic cells, one sees that they decrease with Ra for $Ra \leqslant 10^9$ and appear to reach another plateau around $\langle \sigma_{T,c}/\theta_* \rangle_{Ra,Pr} = 0.34$ afterwards (the lower solid line in figure 3*b*). If this feature can be verified by data for higher Ra, then this means the above constant is cell-geometry-dependent. This dependence may be a result of the different azimuthal dynamics of the large-scale flow in the two geometries. A previous study suggests that the scaling of the r.m.s. temperature depends on cell geometry (Daya & Ecke 2001). Now one sees that $\sigma_{T,c}/\theta_*$ reaches different plateaus in cells with different geometries. It can thus be used to characterise and quantify the level of turbulent fluctuations in different cell geometries. The apparent different behaviours in the bulk fluctuation remain to be explained. We note a potential application of the above result is in cases where it is difficult to measure σ_T directly. In such situations, one can use global quantities such as Ra, Nu and Pr to obtain an estimate of the level of turbulent fluctuations in the core region.

3.2. *The vertical velocity fluctuation in the bulk*

We study the velocity fluctuations in this section. Figure 4(*a*) shows the Reynolds number $Re_{\sigma_{w,c}}$ based on the vertical velocity fluctuation $\sigma_{w,c}$ measured at the centre of the rough cell. For comparison, $Re_{\sigma_{w,c}}$ obtained in smooth cells from Shen *et al.* (1995), Daya & Ecke (2001), Qiu *et al.* (2004) and Shang *et al.* (2008) in cylinders

https://doi.org/10.1017/jfm.2019.667 Published online by Cambridge University Press

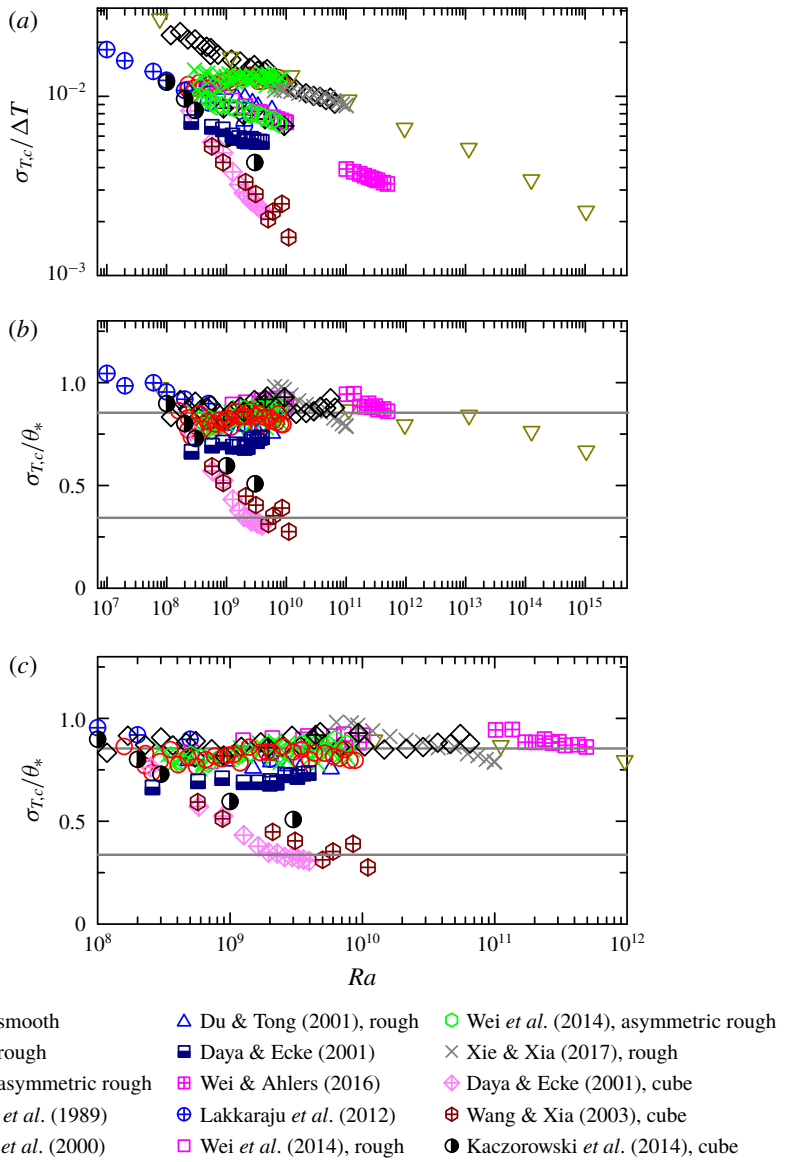


FIGURE 3. (*a*) Normalised r.m.s. temperature at the cell centre $\sigma_{T,c}/\Delta T$ versus Ra. The legends with 'rough' mean rough cells and those with 'cube' means cubic cells. Details of the various data and the associated power laws are given in table 1; (*b*) the same data as in (*a*) but with the vertical axis scaled by θ_*. The upper and lower horizontal lines mark the averaged value of 0.85 in cylindrical cells and 0.34 in cubic cells, respectively. (*c*) A zoom-in of the region with $10^8 \leqslant Ra \leqslant 10^{12}$.

and from Daya & Ecke (2001) and Kaczorowski *et al.* (2014) in cubes are also shown. The $Re_{w,c}$ values in both smooth and rough cells with $\Gamma = 1$ can be described by power laws: $Re_{\sigma_{w,c}} = 0.021 Ra^{0.50\pm0.01}$ (rough cell) and $Re_{\sigma_{w,c}} = 0.014 Ra^{0.50\pm0.01}$ (smooth cell). Note a transition is seen for $Ra \geqslant 10^9$ in the data obtained in a cube by Daya & Ecke (2001), implying a geometry dependence of the velocity fluctuation. As these

https://doi.org/10.1017/jfm.2019.667 Published online by Cambridge University Press

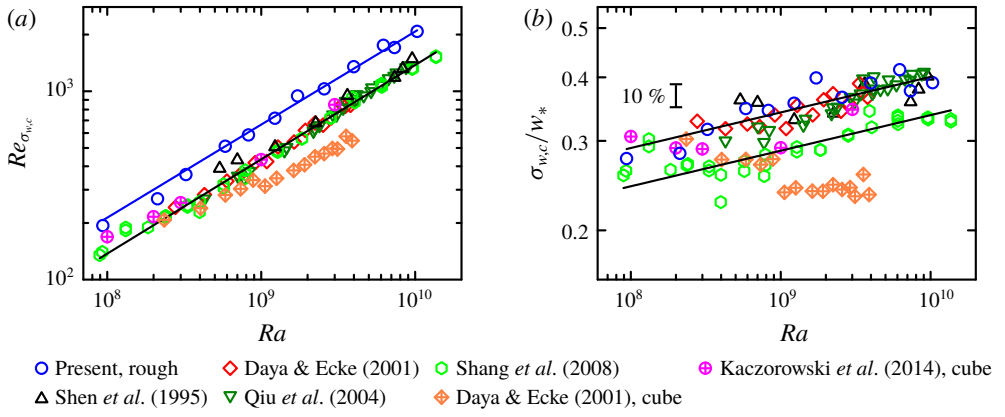


FIGURE 4. (*a*) Measured Reynolds number $Re_{\sigma_{w,c}}$ in a rough cell. $Re_{\sigma_{w,c}}$ values obtained in smooth cells from the literature are also shown. The solid lines are power-law fits to the data, yielding $Re_{\sigma_{w,c}} = 0.021Ra^{0.50\pm0.01}$ (circles, rough cell) and $Re_{\sigma_{w,c}} = 0.014Ra^{0.50\pm0.01}$ (smooth cell). (*b*) Values of $\sigma_{w,c}$ normalised by w_* versus Ra. The two solid lines are power-law fits to the data: $\sigma_{w,c}/w_* = 0.08Ra^{0.07\pm0.02}$ (upper line) and $\sigma_{w,c}/w_* = 0.07Ra^{0.07\pm0.02}$ (lower line).

data are taken in a cell with $\Gamma = 0.7$, they are not used in the fitting. The velocity fluctuations in the rough cell are enhanced by 50 % when compared with those in smooth cells. This directly confirms that not only are the temperature fluctuations enhanced in a rough cell, but also the velocity fluctuations.

To test if the convective velocity w_* is a characteristic scale for velocity in the core region, we study $\sigma_{w,c}/w_*$. The $\sigma_{w,c}/w_*$ data are obtained by first calculating $Re_{\sigma_{w,c}}$, and then Re_{w_*} using (2.1*b*) with Ra, Pr and Nu values that were measured simultaneously with $\sigma_{w,c}$. The ratio between $Re_{\sigma_{w,c}}$ and Re_{w_*} is therefore $\sigma_{w,c}/w_*$. Figure 4(*b*) plots $\sigma_{w,c}/w_*$ versus Ra. For the data from Daya & Ecke (2001), Qiu *et al.* (2004) and Shang *et al.* (2008), there are no Nu data available. To obtain Re_{w*}, we used the heat transport scaling relation $Nu = 0.14Ra^{0.297}Pr^{-0.03}$, which was obtained in the Ra range $2 \times 10^7 \leqslant Ra \leqslant 3 \times 10^{10}$ and the Pr range $4 \leqslant Pr \leqslant 1350$ (Xia, Lam & Zhou 2002). For the rest of the data, $Re_{\sigma_{w,c}}$ and the corresponding Nu were measured simultaneously. Interestingly, the data in rough cells and smooth cells collapse onto each other, suggesting that $\sigma_{w,c}/w_*$ exhibits universal behaviour that is independent of the plate topography. The scaled $\sigma_{w,c}$ shows a rather weak Ra-dependence, given by $\sigma_{w,c}/w_* \sim Ra^{0.07\pm0.02}$, as indicated by the solid lines in the figure. Note that the data from Shang *et al.* (2008) are ∼14 % lower than the others. We currently do not understand this small difference. It may be due to the systematic error introduced when calculating w_*, which involves values of Nu that were not measured simultaneously with $\sigma_{w,c}$.

Next, we examine the profiles of the vertical r.m.s. velocity $\sigma_w(z)$ in the mixing zone. Experimentally, obtaining velocity r.m.s. profiles requires long-time and multi-point measurement. Because of this, experimentally measured profiles of σ_w are scarce. For this reason, we use profiles from numerical studies. Figure 5(*a*) shows the horizontally averaged vertical r.m.s. velocity profiles $\sigma_w(z)$, which are adopted from Scheel & Schumacher (2016). Both Ra and Pr for these profiles vary over a wide range. It is seen that, when normalised by the free-fall velocity U_f, the profiles do not collapse onto a single curve, suggesting that U_f is not a characteristic

https://doi.org/10.1017/jfm.2019.667 Published online by Cambridge University Press

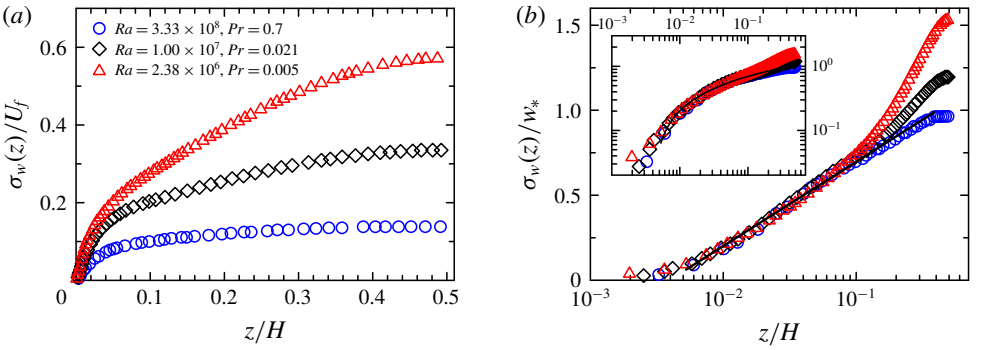


FIGURE 5. Profiles of vertical r.m.s. velocity σ_w. The vertical axes are scaled by (*a*) the free-fall velocity U_f and (*b*) the convective velocity w_*. The solid line in (*b*) is a logarithmic fit to the data in the range $4 \times 10^{-3} \leqslant z/H \leqslant 7 \times 10^{-2}$, yielding $\sigma_w/w_* = 0.22 \ln(z/H) + 1.22$. Inset of (*b*): $\sigma_w(z)/w_*$ in a log–log plot. The data are taken from Scheel & Schumacher (2016).

velocity scale in the bulk. Figure 5(*b*) plots the same data set as those in figure 5(*a*), but with the vertical axis scaled by w_*. The data for different Ra and Pr now collapse onto each other in the mixing zone, suggesting that w_* is a proper velocity scale. The $\sigma_{w,c}/w_*$ data in the range $4 \times 10^{-3} \leqslant z/H \leqslant 7 \times 10^{-2}$ can be fitted by a logarithmic function, given by $\sigma_w/w_* = 0.22 \ln(z/H) + 1.22$. This logarithmic dependence is in agreement with the theoretical prediction by Adrian (1996). It is also observed that the logarithmic region increases with Ra and Pr. The inset of figure 5(*b*) plots the same data as the main figure on a log–log scale, showing that the data cannot be fitted by a power law. Note $\sigma_{w,c}/w_*$ values in the core region are larger than those shown in figure 4(*b*) and they do not collapse onto each other. A possible reason may be that the data presented in figure 4 were taken at a single point (the cell centre), but those in figure 5 were averaged along a horizontal cross-section which includes large velocity fluctuations produced by thermal plumes carried with the large-scale circulation.

3.3. *Implications for ultrahigh-Rayleigh-number convection*

We now study whether the convective temperature is applicable to the ultrahigh-Ra ($\geqslant 10^{13}$) data and may possibly shed some light on the turbulence in this regime. The data are taken from Ahlers *et al.* (2012) with an adapted plot shown in figure 6(*a*). Those data were measured in pressurised SF6 gas with Ra reaching 1×10^{15} and $Pr \approx 0.8$. It is seen that the logarithmic functions fit $\sigma_T(z)/\Delta T$ nicely. But data for different Ra do not collapse, and they seem to have similar decay rates (the pre-factor of the logarithmic term). The observed logarithmic dependence in the plume abundant region, near the sidewall, was also obtained by He & Xia (2019) recently. In figure 6(*b*), we show that once $\sigma_T(z)$ is scaled by θ_*, they fall into two groups. The solid lines in the figure are logarithmic fits to the data in the range $1.8 \times 10^{-2} \leqslant z/H \leqslant 1.46 \times 10^{-1}$, yielding $\sigma_T(z)/\theta_* = -0.49 \ln(z/H) + 1.15$ for $Ra \geqslant 7.90 \times 10^{14}$ and $\sigma_T(z)/\theta_* = -0.30 \ln(z/H) + 1.20$ for $Ra \leqslant 1.18 \times 10^{13}$. The difference in the decay rates suggests that the bulk fluctuations undergo a transition. We note that He *et al.* (2012) have stated that the system has reached the ultimate state of thermal convection for $Ra \geqslant 5 \times 10^{14}$. A systematic investigation on the Ra-dependence of $\theta_T(z)/\theta_*$ could provide more evidence on the existence of an internal flow state transition.

https://doi.org/10.1017/jfm.2019.667 Published online by Cambridge University Press

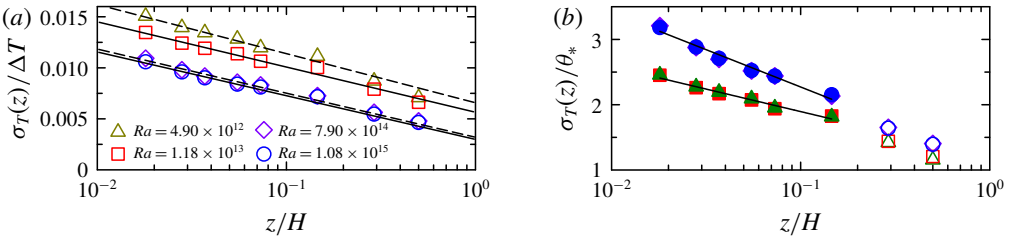


FIGURE 6. The r.m.s. temperature profiles measured in ultrahigh-Ra convection. (a) Figure adapted from Ahlers *et al.* (2012). (b) The same set of data as in (a) with the vertical axis scaled by θ_*. The solid lines in (b) are logarithmic fits to the data with solid symbols: $\sigma_T(z)/\theta_* = -0.49\ln(z/H) + 1.15$ (upper line) and $\sigma_T(z)/\theta_* = -0.30\ln(z/H) + 1.20$ (lower line).

4. Conclusions

We have studied the temperature and the velocity fluctuations in the bulk of Rayleigh–Bénard turbulence using new experimental data from the present study and experimental and numerical data from previous studies. We show that, when scaled by the convective temperature θ_*, the r.m.s. temperature at the cell centre is a constant ($\sigma_{T,c}/\theta_* \approx 0.85$) over the Rayleigh number range of $10^8 \leqslant Ra \leqslant 10^{15}$ and the Prandtl number range of $0.7 \leqslant Pr \leqslant 23.34$, and is independent of the surface topographies of the top and bottom plates of the convection cell. A constant close to unity suggests that the convective temperature is a proper measure of the temperature fluctuations in the core region. The vertical r.m.s. velocity, on the other hand, shows a rather weak Ra-dependence, given by $\sigma_{w,c}/w_* \sim Ra^{0.07\pm0.02}$, which is also independent of the plate topography. In the mixing zone with a mean horizontal shear, the r.m.s. temperature profile $\sigma_T(z)/\theta_*$ obeys a power-law dependence on the vertical distance z from the plate, and the vertical r.m.s. velocity profile $\sigma_w(z)/w_*$ obeys a logarithmic dependence on z. The study thus demonstrates that the typical scales for the temperature and the velocity are the convective temperature θ_* and the convective velocity w_*, respectively. The discovery of these universal aspects of fluctuations sheds new light on the bulk dynamics in convective turbulence. We further show that θ_* could be used to study internal flow state transitions in the ultrahigh-Ra turbulent convection. We note that, despite universal properties holding over a wide range of Ra, Pr and surface topographies, $\sigma_{T,c}/\theta_*$ is found to depend on the cell geometry – it is a constant of 0.34 in cubes and 0.85 in cylinders. The scaling exponent of the σ_T/θ_* profile also depends on the cell geometry. Finally, the present study focuses on turbulent fluctuations in convection cells with an aspect ratio close to unity. It will be interesting to find out if the universal behaviour observed here will also exist in cells of different aspect ratios.

Acknowledgement

We thank S.-D. Huang and Y.-H. He for helpful discussions. This work was supported by a SUSTech Startup Fund and by the Hong Kong Research Grant Council under grant nos CUHK 14301115 and 14302317.

https://doi.org/10.1017/jfm.2019.667 Published online by Cambridge University Press

References

ADRIAN, R. J. 1996 Variation of temperature and velocity fluctuations in turbulent thermal convection over horizontal surfaces. *Intl J. Heat Mass Transfer* **39**, 2303–2310.

AHLERS, G., BODENSCHATZ, E., FUNFSCHILLING, D., GROSSMANN, S., HE, X., LOHSE, D., STEVENS, R. J. A. M. & VERZICCO, R. 2012 Logarithmic temperature profiles in turbulent Rayleigh–Bénard convection. *Phys. Rev. Lett.* **109**, 114501.

AHLERS, G., GROSSMANN, S. & LOHSE, D. 2009 Heat transfer and large scale dynamics in turbulent Rayleigh–Bénard convection. *Rev. Mod. Phys.* **81**, 503–537.

CASTAING, B., GUNARATNE, G., HESLOT, F., KADANOFF, L., LIBCHABER, A., THOMAE, S., WU, X.-Z., ZALESKI, S. & ZANETTI, G. 1989 Scaling of hard thermal turbulence in Rayleigh–Bénard convection. *J. Fluid Mech.* **204**, 1–30.

CHILLÀ, F. & SCHUMACHER, J. 2012 New perspectives in turbulent Rayleigh–Bénard convection. *Eur. Phys. J.* E **35**, 58.

DAYA, Z. A. & ECKE, R. E. 2001 Does turbulent convection feel the shape of the container? *Phys. Rev. Lett.* **87**, 184501.

DEARDORFF, J. W. 1970 Convective velocity and temperature scales for the unstable planetary boundary layer and for Rayleigh convection. *J. Atmos. Sci.* **27**, 1211–1213.

DU, Y. B. & TONG, P. 2000 Turbulent thermal convection in a cell with ordered rough boundaries. *J. Fluid Mech.* **407**, 57–84.

DU, Y. B. & TONG, P. 2001 Temperature fluctuations in a convection cell with rough upper and lower surfaces. *Phys. Rev.* E **63**, 046303.

GROSSMANN, S. & LOHSE, D. 2004 Fluctuations in turbulent Rayleigh–Bénard convection: the role of plumes. *Phys. Fluids* **16**, 4462–4472.

HE, X., FUNFSCHILLING, D., NOBACH, H., BODENSCHATZ, E. & AHLERS, G. 2012 Transition to the ultimate state of turbulent Rayleigh–Bénard convection. *Phys. Rev. Lett.* **108**, 024502.

HE, Y.-H. & XIA, K.-Q. 2019 Temperature fluctuation profiles in turbulent thermal convection: a logarithmic dependence versus a power-law dependence. *Phys. Rev. Lett.* **122**, 014503.

HESLOT, F., CASTAING, B. & LIBCHABER, A. 1987 Transitions to turbulence in helium gas. *Phys. Rev.* A **36**, 5870–5873.

KACZOROWSKI, M., CHONG, K.-L. & XIA, K.-Q. 2014 Turbulent flow in the bulk of Rayleigh–Bénard convection: aspect-ratio dependence of the small-scale properties. *J. Fluid Mech.* **747**, 73–102.

LAKKARAJU, R., STEVENS, R. J. A. M., VERZICCO, R., GROSSMANN, S., PROSPERETTI, A., SUN, C. & LOHSE, D. 2012 Spatial distribution of heat flux and fluctuations in turbulent Rayleigh–Bénard convection. *Phys. Rev.* E **86**, 056315.

LOHSE, D. & XIA, K.-Q. 2010 Small-scale properties of turbulent Rayleigh–Bénard convection. *Annu. Rev. Fluid Mech.* **42**, 335–364.

LUI, S.-L. & XIA, K.-Q. 1998 Spatial structure of the thermal boundary layer in turbulent convection. *Phys. Rev.* E **57**, 5494–5503.

NIEMELA, J. J., SKRBEK, L., SREENIVASAN, K. R. & DONNELLY, R. J. 2000 Turbulent convection at very high Rayleigh numbers. *Nature* **404**, 837–840.

QIU, X. L., SHANG, X.-D., TONG, P. & XIA, K.-Q. 2004 Velocity oscillations in turbulent Rayleigh–Bénard convection. *Phys. Fluids* **16**, 412–423.

SCHEEL, J. D. & SCHUMACHER, J. 2016 Global and local statistics in turbulent convection at low Prandtl numbers. *J. Fluid Mech.* **802**, 147–173.

SHANG, X.-D., TONG, P. & XIA, K.-Q. 2008 Scaling of the local convective heat flux in turbulent Rayleigh–Bénard convection. *Phys. Rev. Lett.* **100**, 244503.

SHEN, Y., XIA, K.-Q. & TONG, P. 1995 Measured local-velocity fluctuations in turbulent convection. *Phys. Rev. Lett.* **75**, 437–440.

SUN, C., CHEUNG, Y.-H. & XIA, K.-Q. 2008 Experimental studies of the viscous boundary layer properties in turbulent Rayleigh–Bénard convection. *J. Fluid Mech.* **605**, 79–113.

WANG, J. & XIA, K.-Q. 2003 Spatial variations of the mean and statistical quantities in the thermal boundary layers of turbulent convection. *Eur. Phys. J.* B **32**, 127–136.

https://doi.org/10.1017/jfm.2019.667 Published online by Cambridge University Press

WANG, Y., XU, W., HE, X., YIK, H., WANG, X., SCHUMACHER, J. & TONG, P. 2018 Boundary layer fluctuations in turbulent Rayleigh–Bénard convection. *J. Fluid Mech.* **840**, 408–431.

WEI, P. & AHLERS, G. 2016 On the nature of fluctuations in turbulent Rayleigh–Bénard convection at large Prandtl numbers. *J. Fluid Mech.* **802**, 203–244.

WEI, P., CHAN, T.-S., NI, R., ZHAO, X.-Z. & XIA, K.-Q. 2014 Heat transport properties of plates with smooth and rough surfaces in turbulent thermal convection. *J. Fluid Mech.* **740**, 28–46.

XIA, K.-Q. 2013 Current trends and future directions in turbulent thermal convection. *Theor. Appl. Mech. Lett.* **3**, 052001.

XIA, K.-Q., LAM, S. & ZHOU, S.-Q. 2002 Heat-flux measurement in high-Prandtl-number turbulent Rayleigh–Bénard convection. *Phys. Rev. Lett.* **88**, 064501.

XIE, Y.-C., DING, G.-Y. & XIA, K.-Q. 2018 Flow topology transition via global bifurcation in thermally driven turbulence. *Phys. Rev. Lett.* **120**, 214501.

XIE, Y.-C. & XIA, K.-Q. 2017 Turbulent thermal convection over rough plates with varying roughness geometries. *J. Fluid Mech.* **825**, 573–599.

https://doi.org/10.1017/jfm.2019.667 Published online by Cambridge University Press